

Existence of a photonic band gap in two dimensions

Robert D. Meade, Karl D. Brommer, Andrew M. Rappe, and J. D. Joannopoulos
Department of Physics, Massachusetts Institute of Technology, Cambridge, Massachusetts 02139

(Received 13 December 1991; accepted for publication 28 May 1992)

A systematic theoretical investigation is undertaken in order to identify a two-dimensional periodic dielectric structure that has a complete in-plane photonic band gap for both polarizations. Of the various structures studied, only a triangular lattice of air columns is found to have the desired band-gap properties. Microwave transmission experiments are performed to test the theoretical predictions.

Since the first suggestion that a dielectric material with three-dimensional (3D) periodicity could reflect light incident from any direction, there has been rapid progress in the newly emergent field of photonic band-gap materials.¹⁻⁹ Several structures which exhibit a photonic band gap have been discovered^{5,6} and a number of important properties of these materials, such as the localization of light at defects^{7,8} and surfaces,⁹ have been discussed. The related problem of dielectric crystals which have a two-dimensional (2D) periodicity in the \hat{x} - \hat{y} plane and are continuous in the \hat{z} direction is also beginning to receive some attention.¹⁰⁻¹³

In previous work,^{10,11} dielectric structures which had band gaps for individual polarizations were found. In this letter, we present a 2D structure in which these band gaps overlap to form a complete gap which prevents the in-plane propagation of light of any polarization. We first employ theoretical calculations to discover such a system and then perform microwave transmission experiments to verify that light of any polarization cannot propagate in this structure. While this work concentrates on the propagation of light in the 2D plane, we conclude this letter by discussing the out-of-plane photonic band structure.

In a 2D photonic crystal, like its 3D counterpart, the light propagates as Bloch waves, $\mathbf{H}(\mathbf{r}) = \mathbf{u}(\mathbf{r})e^{i\mathbf{k}\cdot\mathbf{r}}$. To understand this propagation let us consider the reciprocal space of a 2D system. Since the crystal has discrete translational symmetry in the \hat{x} - \hat{y} plane, there is a finite in-plane Brillouin zone described by in-plane wave vectors k_1, k_2 with $(-G_1/2) < k_1 < (G_1/2)$ and $(-G_2/2) < k_2 < (G_2/2)$, where G_1, G_2 are the reciprocal lattice vectors. In the \hat{z} direction, however, the system is continuous and so the wave vector can assume any value $-\infty < k_z < \infty$. Since the system has no index contrast in the \hat{z} direction, a wave traveling in this direction is not scattered. Thus, we argue on physical grounds that there cannot be a band gap for light propagating in the \hat{z} direction with $k_1 = k_2 = 0$. In the first part of this letter, we will restrict our attention to the in-plane band structure $k_z = 0$. With this assumption, we can take advantage of the mirror symmetry to restrict the fields as either odd or even under M_x . Thus we can catalog the electromagnetic modes as one of two types, either (H_x, H_y, E_z) or (E_x, E_y, H_z) which we will refer to as E perpendicular to the plane or E parallel to the plane, respectively.

In order to calculate the electromagnetic frequency spectrum of these dielectric lattices, we have employed the computational techniques described in Refs. 3-5. Briefly,

the macroscopic Maxwell's equations can be rearranged to yield the eigenvalue equation $\nabla \times (1/\epsilon(\mathbf{r})\nabla \times \mathbf{H}) = (\omega^2/c^2)\mathbf{H}$. The magnetic field $\mathbf{H}(\mathbf{r})$ can be expressed as a sum of plane waves

$$\mathbf{H}(\mathbf{r}) = \sum_{\mathbf{G}} \sum_{\lambda=1,2} h_{\mathbf{G},\lambda} \hat{\mathbf{e}}_{\lambda} e^{i(\mathbf{k}+\mathbf{G})\cdot\mathbf{r}},$$

where \mathbf{k} is in the Brillouin zone, \mathbf{G} is summed over the reciprocal lattice, and $\hat{\mathbf{e}}_{\lambda}$ are polarizations orthogonal to $(\mathbf{k} + \mathbf{G})$. By limiting the size of the wave vector included in this plane-wave expansion, a finite sum is achieved. The eigenvalue equation is now expressed in matrix form

$$\sum_{\mathbf{G}',\lambda'} H_{\mathbf{G},\mathbf{G}'}^{\lambda\lambda'} h_{\mathbf{G}',\lambda'} = \omega^2 h_{\mathbf{G},\lambda},$$

where

$$H_{\mathbf{G},\mathbf{G}'} = |\mathbf{k} + \mathbf{G}| |\mathbf{k} + \mathbf{G}'| \epsilon_{\mathbf{G},\mathbf{G}'}^{-1} \begin{pmatrix} \hat{\mathbf{e}}_2 \cdot \hat{\mathbf{e}}_2' & -\hat{\mathbf{e}}_2 \cdot \hat{\mathbf{e}}_1' \\ -\hat{\mathbf{e}}_1 \cdot \hat{\mathbf{e}}_2' & \hat{\mathbf{e}}_1 \cdot \hat{\mathbf{e}}_1' \end{pmatrix}$$

and $\epsilon_{\mathbf{G},\mathbf{G}'}^{-1}$ is the Fourier transform of the dielectric function $\epsilon(\mathbf{r})$. This eigenvalue equation can now be solved by standard numerical techniques yielding the normal mode coefficients and frequencies of the electromagnetic modes. Because of the 2D nature of the problems considered, plane-wave convergence was achieved with a relatively small number of plane waves and we estimate that by including ~ 140 plane waves per polarization the electromagnetic mode frequencies were obtained to better than 1%. This technique provides a simple and powerful method to solve problems in electrodynamics which takes full account of the vector nature of the electromagnetic radiation.

As in the 3D case, our primary objective is to create a dielectric system which exhibits a complete photonic band gap, a set of frequencies in which light of any polarization cannot propagate in any in-plane direction. In order to find such a structure, we searched all filling fractions of square, triangular, and honeycomb lattices. We also considered dielectric rods in air, as well as air columns drilled in dielectric. At the dielectric contrast of GaAs ($\epsilon = 13$), the only combination which was found to have a photonic band gap in both polarizations was the triangular lattice of air columns in dielectric (see Fig. 1). The maximum band gap we find is $\omega_{\text{gap}}/\omega_{\text{midgap}} = 18.6\%$, which occurs when the radius of the air columns was $r_{\text{max}} = 0.48a$, where a is the in-plane lattice constant. A gap appears in this structure for dielectric contrast of 7.2 or greater (see Fig. 2). This photonic band gap is somewhat unusual because it occurs between

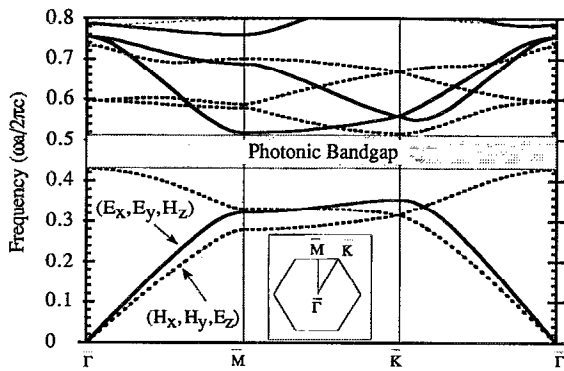


FIG. 1. Frequencies of the lowest photonic bands for a triangular lattice of air columns ($\epsilon_{\text{air}}=1$) drilled in dielectric ($\epsilon_d=13$). The band structure is plotted along special directions of the in-plane Brillouin zone ($k_z=0$), as shown in the lower inset. The radius of the air columns is $r=0.48a$, where a is the in-plane lattice constant. The solid (dashed) lines show the frequencies of bands which have the electric field parallel(perpendicular) to the plane. Notice the photonic band gap between the third and fourth bands.

the third and fourth bands, whereas the photonic band gaps in 3D structures have always occurred between the second and third bands.

We verified our theoretical predictions by constructing a 2D photonic band-gap material from a dielectric block and measuring its transmissivity. We fabricated the sample from a piece of C-Stock 265 manufactured by Cuming Corp. This material consists of glass spheres and aluminum flake mixed in a binder to give an artificial dielectric with a constant $\epsilon \approx 13-15$ (we assume $\epsilon=13$). This material was chosen because it was inexpensive and easy to machine. Using a numerically controlled drill, the sample could be constructed in about 4 h. An 8×14 array of air columns of diameter 0.992 cm were drilled in a triangular lattice with lattice constant 1.044 cm and so $r/a=0.475$, close to the

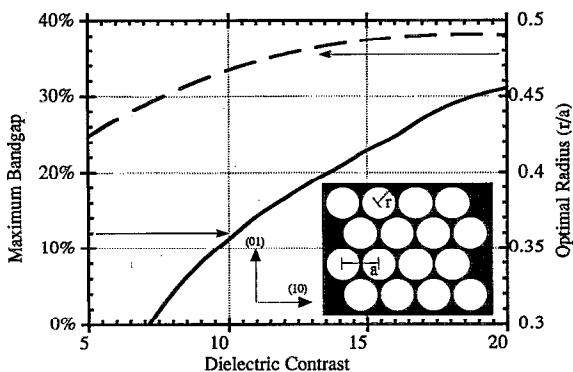


FIG. 2. The maximum photonic band gap achievable for different dielectric contrast (solid line), and the optimal radius for which the maximum band gap is achieved (dashed line). The band gap is expressed as a percentage of the midgap frequency, and the radius in units of the lattice constant. Note that the band gap first appears at a dielectric contrast of 7.2.

optimal theoretical ratio. Based on our calculations, we expected a gap in the range 12.3–14.6 GHz.

We performed free-space transmission measurements at an antenna test range. We mounted the photonic band gap material inside a 7.5 by 15 cm aperture cut into a 90×90 cm sheet of radar absorbing material. A broadband horn antenna illuminated the sample at a range of 5.5 m. The 3 dB beamwidth of the radiated pattern was 60 cm at this range, ensuring flat, plane-wave illumination across the full extent of the sample. A notch antenna mounted directly behind the sample received the transmitted signal. An HP8510 network analyzer measured the power transmitted between the antennas. We used a chirped wave form along with digital range gating to eliminate extraneous reflections from objects near the sample. The sensitivity of our system was measured at 70 dB. This level of dynamic range enabled us to study detailed structure inside the photonic band gap, especially to compare the transmitted power of different photonic band gaps. Transmission amplitude was measured from 2 to 18 GHz at different sample orientations as the sample was rotated on an antenna pedestal. Both polarizations were studied by rotating the antennas. Two separate pairs of antennas were required to cover the entire 2–18 GHz range.

In Fig. 3, we display the experimental transmission spectrum $T(\omega, k_{\parallel})$ and the calculated band structure of our 2D structure. Note that there is no transmission for either polarization in the electromagnetic band gap, between 13 and 15.5 GHz. We anticipate if there are electromagnetic modes at (ω, k_{\parallel}) , then the light will travel through the sample and the transmission $T(\omega, k_{\parallel})$ will be large. On the other hand, if the density of states is zero at (ω, k_{\parallel}) , then the light will decay into the sample and $T(\omega, k_{\parallel})$ will be greatly reduced. These expectations are fulfilled in Fig. 3(a), which shows the transmission spectrum for light which is polarized with electric field normal to the plane. As we can see in this figure, the transmission is large (light regions) in area where there are traveling modes (shaded by vertical lines). In the gap, however, the fields are strongly attenuated (dark regions) with transmission dropping by five orders of magnitude.

Figure 3(b) shows the transmission spectrum for light which is polarized with electric field perpendicular to the plane. This polarization has two gaps, a complete gap at 13 GHz, and a minigap at 8.5 GHz. The attenuation is small for the minigap, with the transmission dropping only by 20 dB. The complete gap begins at 12.5 GHz, as we expect theoretically, and the attenuation remains large (~ 50 dB) until 18 GHz, which is the limit of our experimental resolution. However, we expect theoretically that the material should transmit light via the band centered at 16 GHz. Although this seems puzzling, it is quite similar to the results of Robertson *et al.*¹³ These authors found that symmetry constraints prevented certain bands from transmitting light which was incident as a plane wave.

Until this point, we have considered only the case in which light propagates in the 2D plane ($k_z=0$). However, for some applications it is important to understand the out-of-plane band structure, shown in Fig. 4. The inset to

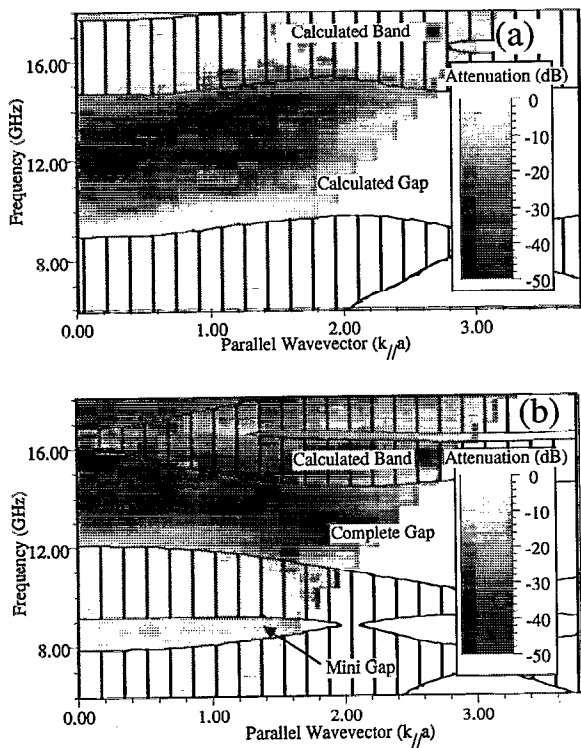


FIG. 3. The transmission spectrum of our 2D structure for light polarized with electric field parallel to the 2D plane (a) and perpendicular to the 2D plane (b). The transmission amplitude $T(\omega, k_{\parallel})$ is plotted for different frequencies and parallel wave vectors. The attenuation is displayed in grey scale, with the light regions representing large transmission and the dark regions representing large attenuation. Variations in the attenuation are due to reflection, not absorption. Note that there is no transmission for either polarization in the electromagnetic band gap, between 13 and 16 GHz. Because the sample was illuminated along the (01) face (see Fig. 2, inset), the parallel wave vector refers to variation in the (10) direction. The vertical lines in the figure designate the regions of (ω, k_{\parallel}) in which calculations find electromagnetic modes. These modes may have any wave vector along the (01) direction, but have $k_z=0$.

this figure shows the frequency dependence of the lowest band as k_z is varied. When $k_z=0$, this lowest band spans a broad range of frequencies (see Fig. 1). However, in the inset to Fig. 4 we see that as k_z increases the lowest band becomes flat, and so the in-plane bandwidth tends to zero. Figure 4 also plots the frequency of the lowest six bands as k_z is varied. It shows both $\omega(\bar{\Gamma}, k_z)$ and $\omega(\bar{K}, k_z)$, corresponding to the frequency change of the bands which start at $\bar{\Gamma}$ and \bar{K} , respectively. Clearly, as k_z increases the bandwidth of each of the photonic bands tends towards zero.

Thus, the primary feature of the out-of-plane band-structure is that as k_z increases, the in-plane bandwidth tends to zero. We can understand this simply. For large k_z , the light is totally internally reflected inside the dielectric regions, just as in an optical waveguide. Because there is very little overlap between light trapped in neighboring dielectric waveguides, the modes are decoupled and so the bandwidth tends to zero. This is especially true for modes which have $\omega < ck_z$. Recall that in the vacuum region, light obeys the wave equation $\nabla^2 \mathbf{H} = -(\omega^2/c^2)\mathbf{H}$. If the fields oscillate along the z axis $\mathbf{H}(\mathbf{r}) = \mathbf{u}(x, y)e^{ik_z z}$, then the wave equation reduces to $\nabla_{\parallel}^2 \mathbf{u} = [k_z^2 - (\omega^2/c^2)]\mathbf{u}$. Thus, if $\omega < ck_z$ then the fields are strongly exponentially decaying in the

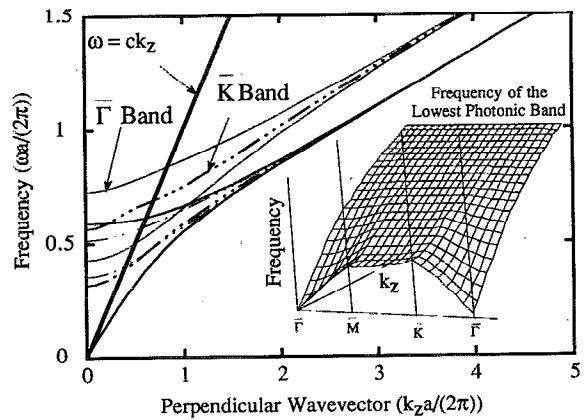


FIG. 4. The out-of-plane band structure of the triangular lattice of air columns. The frequencies of the lowest six bands are shown vs k_x . The frequencies of the bands which start at $\bar{\Gamma}$, $\omega(\bar{\Gamma}, k_z)$, are plotted using solid lines, whereas the frequencies of the bands which start at \bar{K} , $\omega(\bar{K}, k_z)$, are plotted using dashed-dotted lines. The thick (thin) lines correspond to doubly (singly) degenerate modes. The straight line $\omega = ck_z$ separates the regions in which the modes are oscillatory ($\omega > ck_z$) in the air regions from those which are evanescent ($\omega < ck_z$) in the air regions. The inset to this figure shows the frequency dependence of the lowest band as k_z is varied. Note that as k_z increases the lowest band becomes flat.

vacuum region, and so the overlap between modes in neighboring regions of dielectric vanishes, and the bandwidth goes to zero. The bands in Fig. 4 display this behavior. Above the light cone $\omega > ck_z$, the bands have a large dispersion, while for $\omega < ck_z$ this bandwidth goes to zero.

Note added in proof: Since submission, another group¹⁴ has reported the existence of a band gap common to both polarizations for a square lattice of air columns in dielectric. This band gap is appreciable at large index contrast and vanishes at $\epsilon = 12.3$.

The experiments were funded by Lockheed Sanders. We thank R. Gilbert and H. Mullaney for helpful discussions and D. Larochelle for assisting in designing the experiment. Partial support for this work was provided by the Office of Naval Research Contract No. N00014-90-J-1370. Finally, one of us (A.M.R.) would like to acknowledge the support of the Joint Services Electronics Program.

- ¹E. Yablonovitch, Phys. Rev. Lett. **58**, 2059 (1987).
- ²E. Yablonovitch and T. J. Gmitter, Phys. Rev. Lett. **63**, 1950 (1989).
- ³K. M. Leung and Y. F. Liu, Phys. Rev. Lett. **65**, 2646 (1990).
- ⁴Z. Zhang and S. Satpathy, Phys. Rev. Lett. **65**, 2650 (1990).
- ⁵K. M. Ho, C. T. Chan, and C. M. Soukoulis, Phys. Rev. Lett. **65**, 3125 (1990).
- ⁶E. Yablonovitch, T. J. Gmitter, and K. M. Leung, Phys. Rev. Lett. **67**, 2295 (1991).
- ⁷R. D. Meade, K. D. Brommer, A. M. Rappe, and J. D. Joannopoulos, Phys. Rev. B **44**, 13772 (1991).
- ⁸E. Yablonovitch, T. J. Gmitter, R. D. Meade, K. D. Brommer, A. M. Rappe, and J. D. Joannopoulos, Phys. Rev. Lett. **67**, 3380 (1991).
- ⁹R. D. Meade, K. D. Brommer, A. M. Rappe, and J. D. Joannopoulos, Phys. Rev. B **44**, 10961 (1991).
- ¹⁰M. Plihal, A. Shambrook, A. A. Maradudin, and P. Sheng, Opt. Commun. **80**, 199 (1991).
- ¹¹M. Plihal and A. A. Maradudin, Phys. Rev. B **44**, 8586 (1991).
- ¹²S. L. McCall, P. M. Platzman, R. Dalichaouch, D. Smith, and S. Schultz, Phys. Rev. Lett. **67**, 2017 (1991).
- ¹³W. Robertson, G. Arjavalingam, R. D. Meade, K. D. Brommer, A. M. Rappe, and J. D. Joannopoulos, Phys. Rev. Lett. **68**, 2023 (1992).
- ¹⁴P. Villeneuve and M. Piche, Phys. Rev. B (to be published).